УДК 621.791

FORCE CONTROL STRATEGIES TO REDUCE WELD DISTORTION AND COLD CRACKING IN LASER BEAM WELDING

Wasilewski E., M.Sc., research associate
Brandenburg University of Technology Cottbus-Senftenberg

Abstract. *In recent years, lightweight construction and the demand for resource and energy efficiency have increasingly supported the use of high-strength steels. Laser beam welding (LBW) of these materials is used in industrial mass production to efficiently manufacture high-precise components and parts with the highest quality requirements. Avoiding welding-related defects such as weld distortion and cold cracking is critical. Conventional applications currently meet this requirement to a limited extent due to very restricted process tolerances and the use of non-critical materials, which limits the potential of the joining process. Based on FE welding process simulations, concepts have been developed to reduce distortion and cracking through active control of the LBW process. The underlying models consider the weld induced temperature field, microstructure transformations, and residual stresses to calculate distortion. In addition, the local hydrogen concentration is calculated, and the results of the welding process simulation are evaluated using a cold cracking tool that includes material-specific cracking criteria. The ability to simulate distortion and cold cracking behavior opens up the possibility of parameter variation. From the data collected, concepts of active force introduction with dynamic workpiece clamping have been derived that lead to distortion and cold cracking reduction and promote the weldability of high-strength materials.*
Keywords: *Laser beam welding, High-strength steel, Weld Distortion, Cold-Cracking, Finite element welding simulations*

СТРАТЕГІЇ КЕРУВАННЯ ЗУСИЛЛЯМ ДЛЯ ЗМЕНШЕННЯ ВИКРИВЛЕННЯ ЗВАРНОГО ШВА І ХОЛОДНОГО РОЗТРІСКУВАННЯ ПРИ ЛАЗЕРНОМУ ЗВАРЮВАННІ

Wasilewski E., магістр наук., науковий співробітник
Бранденбурзький технічний університет Котбус-Зенфтенберг

Анотація. *Останніми роками будівництво і попит на ресурсо- та енергоефективність дедалі більше сприяють використанню високоміцних сталей. Лазерне променеве зварювання (ЛПЗ) цих матеріалів використовується в промисловому масовому виробництві для ефективного виготовлення високоточних компонентів і деталей з найвищими вимогами до якості. Уникнення дефектів, пов'язаних зі зварюванням, таких як викривлення шва і холодне розтріскування, має вирішальне значення. Традиційні способи зварювання в даний час відповідають цій вимозі в обмеженій мірі через дуже жорсткі технологічні допуски і використання некритичних матеріалів, що обмежує потенціал процесу з'єднання. На основі моделювання процесу зварювання методом кінцевих елементів були розроблені концепції зменшення викривлення та розтріскування за рахунок активного керування процесом зварювання під флюсом. Основні моделі враховують індуковане зварювальним швом температурне поле, перетворення мікроструктури та залишкові напруження для розрахунку викривлення. Крім того, розраховується локальна концентрація водню, а результати моделювання процесу зварювання оцінюються за допомогою інструменту холодного розтріскування, який включає критерії розтріскування, специфічні для конкретного матеріалу. Здатність моделювати деформацію і поведінку холодного розтріскування відкриває можливість варіювання параметрів. На основі отриманих даних розроблено концепції прикладання активної сили з динамічним затисканням заготовки, які призводять до зменшення деформації та холодного розтріскування і сприяють зварюваності високоміцних матеріалів.*

Ключові слова: *зварювання лазерним променем, Високоміцна сталь, Викривлення зварного шва, Холодне розтріскування, Моделювання зварювання методом скінченних елементів.*

Introduction

To achieve the quality standards and economic productivity required for Laser Beam Welding (LBW), it is essential to prevent welding-related defects like distortion and cracking, particularly in the context of industrial mass production. Active process control for reducing distortion and cracking has not been technically implemented jet, as these issues emerge after the welding process. Consequently, maintaining the required quality standards relies heavily on the strict tolerances of the components being welded. Furthermore, the utilization of high-strength materials is restricted due to their moderate weldability, preventing their full potential from being realized.

This study shows the development of a simulation-controlled process that employs dynamic workpiece clamping for precise force application during LBW. The aim is to develop concepts that guarantee excellent weld quality with minimal distortion, specifically focusing on the prevention of defects such as cold cracking. The methodical approach considers three key components: Finite Element (FE) welding simulation, cold crack prediction using a specialized tool, and process control using a clamping device with dynamically adjustable axes (as shown in the left portion of Figure 1). To accurately calculate distortion, it is essential to perform a combined thermo-metallurgical and thermo-mechanical analysis that considers both welding parameters and microstructure-dependent material properties. Cold cracking typically occurs during the cooling phase of a hardened structure in regions with high tensile stress and increased hydrogen concentrations. As such, the simulation also models the distribution of diffusible hydrogen. To assess the cold cracking susceptibility, the relevant influencing factors (heating rate, maximum temperature, cooling time, stresses, and hydrogen concentration) for all regions of the weld and heat-affected zone (HAZ) are analyzed using a coupled cold cracking tool. This tool is used in conjunction with a material-specific cold cracking criterion, as illustrated in Figure 1 within Chapters 2 and 3. By considering these factors, the approach aims to minimize the risk of cold cracking and improve overall weld quality.

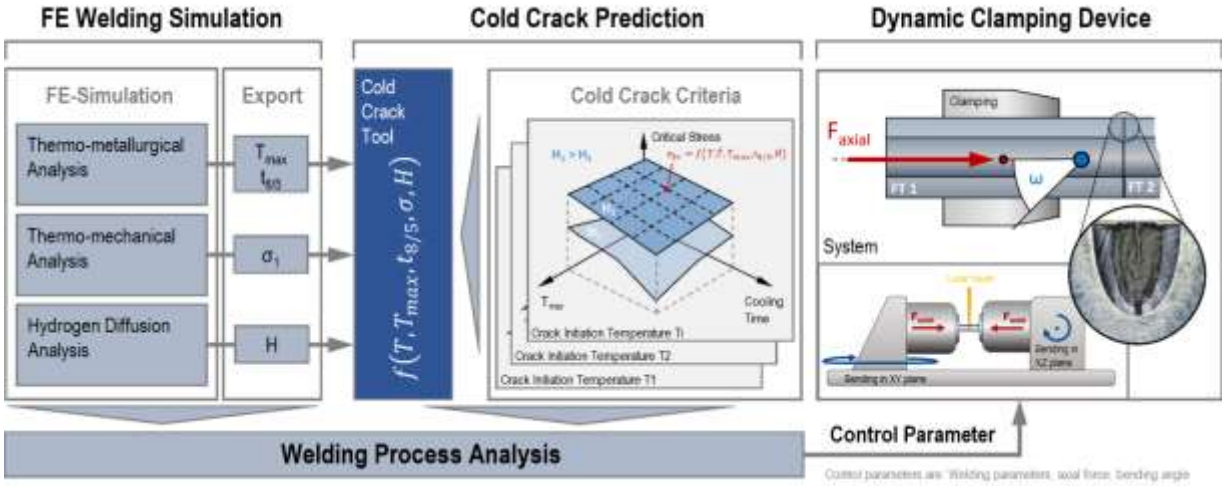

Fig. 1. Three components: FE welding simulation, cold crack prediction using a cold crack tool

A dynamic clamping device, depicted in the right section of Figure 1, enables the application of time-varying axial forces and torques during the LBW process by adjusting a specific axis. The optimized control variables for mitigating cold cracking and distortion are derived from the simulations.

Analysis of Publications

Laser beam welding represents a cutting-edge welding technology that utilizes a highly focused and intense beam of monochromatic light as the energy source for welding. The focused nature of the laser beam enables precise control over the amount of energy applied to the material, resulting in a highly efficient and accurate welding process. LBW can be performed at high speeds, providing a significant advantage in terms of reducing the time and cost associated with welding operations. [1, 2]

In the automotive sector, LBW is widely used to join crucial components of vehicles, such as body panels, exhaust systems, and engine parts, as it results in stronger and more visually appealing welds. Coviello et al. [3] introduced a new method for joining Al-Si-coated blanks in automotive applications using a filler wire and laser optics with variable energy distribution. This approach resulted in high tensile strength and hardness while being stable, reliable, and suitable for production. Nayak et al. [4] covers the use of laser welding for advanced high-strength steels (AHSS) in automotive applications, highlighting its benefits in reducing weight and improving fuel efficiency. The aerospace industry also highly values LBW for its ability to produce high-quality, reliable welds that meet tight tolerances and minimize distortion, making it the preferred choice for welding critical aircraft components such as landing gear, engine parts, and turbine blades. Wen et al. [5] examine the formation of porosity and burn through holes in laser welding of titanium alloys in aerospace, considering different welding positions and parameters. With support of numerical simulations, the study finds that low heat input can reduce burn through holes in the vertical up position, while higher laser power and speed can reduce porosity in the vertical down position.

To address the problem of distortions in LBW, a number of control strategies have been developed to reduce it. Fahlström et al. [6] present a study that investigates the impact of laser welding on the distortion of ultra-high-strength steels in the automotive industry. The study identifies key parameters that influence the magnitude and distribution of distortions and provides effective measures to minimize them, for example, by adjusting the welding speed or the clamping setup. Babu et al. [7] studied the effect of aluminum heat sink and cooling medium on laser welding of duplex stainless steel. The results show that the use of a heat sink has a positive effect on distortion, while slower cooling rates in air quenching result in higher tensile strength. The objective of the study is to experimentally analyze the effect of cooling medium and heat sink on the mechanical and metallurgical properties of laser-welded duplex stainless steel. One of the most effective strategies is active force control, where an external force is introduced during the welding process to counteract the forces causing distortion. Schricker et al. [8], for example, developed an adaptive clamping device for laser-beam welding in a butt-joint configuration. The device uses sensors and actuators to acquire data and adjust the process conditions and workpiece position during welding.

Cold cracking is another major issue in LBW caused by hydrogen in the weld zone. High-strength steels are particularly vulnerable to this issue due to their increased hardness and tensile stresses [9]. Velasquez et al. [10] assess the risk of hydrogen-induced cracking (HIC) in safety-relevant SA-508 pressure vessels. The study aims to eliminate the 48-hour hold time requirement before non-destructive testing. The results show that the HIC susceptibility is ranked by the time to failure and sustained mechanical energy, highlighting the importance of proper testing to prevent potential failures in pressure vessels. To address the problem of cold cracking in LBW, the use of test procedures and simulations can be effective in reducing the susceptibility to cold cracking. Kannengiesser and Boellinghaus [11] provide an overview of current technologies and applications for assessing cold cracking susceptibility in welded joints. They evaluate the most important and internationally established tests, classifying them into self-restraint and externally loaded tests. The study covers both metallurgical weldability tests and advanced test methods for evaluating cold cracking susceptibility. It also presents numerical analyses for calculating the restraint intensity as a definitive factor affecting cold cracking. Simulations can be used to predict the hydrogen concentration in the weld zone and to understand the sources of hydrogen in the material. This information can be used to optimize the process parameters, such as laser power and speed, and to develop new strategies to reduce the risk of cold cracking [12]. Steppan et al. [13] study the risk of HIC in T-joints with fillet welds made from high-strength structural steels. They simulate the diffusion behavior and effectiveness of different

post-weld heat treatments to eliminate cracking. The simulation shows that HIC can be avoided by applying post-weld heat treatment.

By coupling temperature field, microstructure and mechanics calculations with diffusion analysis, the hydrogen distribution can be calculated. According to the Gorsky effect, hydrogen diffuses via interstitial sites from regions of contraction to regions of expnaion. This is a time and distance dependent transient process (second Fick's law). Thereby, the concentration gradient is not constant, contrary to the first Fick's law. For the mathematical formulation of the diffusion process, permeability and solubility are material dependent. Using pipeline welds as an application Zhao et al. [14] describe that for X90 steel, it is mainly residual stresses that lead to hydrogen accumulation, while the change in microstructure leads to a reduction in the fusion zone. Diaz et al. [15] show that the diffusible hydrogen distribution in lattice sites follows the tendency of hydrostatic stresses near a crack tip in welded joints. They also state that microstructural influences lead to high concentrations of trapped hydrogen. Rhode et al. [16] describe the influence of hydrogen traps on TIG welded joints of low alloy steel T24. According to them, traps increase the solubility and decrease the diffusion rate. However, trap effects can also be neglected. For example, Boellinghaus et al. show that the ductility of the weld microstructure is reduced by hydrogen uptake and diffusion into crack-critical regions when welding pipelines of supermartensitic steel [17]. In [18], using a trap-free model, they also show that hydrogen diffusion is strongly geometry dependent, so that a correlation between hydrogen diffusion and layer thickness can be observed in multi-layer welding. Stadtaus et al. also neglected trapping phenomena in the FE simulation of the Tekken [19] and CTS [20] cold crack tests and found, for example, that pre- and post-heating can significantly reduce the hydrogen concentration in tensile stress zones.

In summary, LBW is a state-of-the-art technology that offers numerous advantages in various industries, however, improvements in the development of high-strength steels are necessary to further optimize the process. To achieve this, it is important to focus on reducing distortions and weld defects, such as cold cracks, through the use of tailored test methods and numerical simulations.

Methods

Experimental Setup

Axially symmetric hollow cylinders (heat-treated material 100Cr6) with a wall thickness of 2 mm, an outer diameter of 8 mm and a total length of 60 mm were welded into a butt joint with a 360° circumferential radial seam. The distance between the chuck and the center of the weld was 10 mm on both sides of the weld A welding speed of 1 m/min, a laser power of 300 W, and a focal spot of 100 µm were employed during the process. To validate the temperature field calculation, type K thermocouples with a wire diameter of 0.1 mm were used to record temperatures in areas of high and low gradients at a welding angle of 180°. The final distortion of the welded specimens was measured using a MarForm MMQ 400 coordinate measuring machine. The hydrogen content of the welded specimens was analyzed through carrier gas extraction using a JUWE H-mat 225 instrument. These measurements were previously validated with certified samples and defined hydrogen contents (BAM ZRM steel H1), resulting in an initial hydrogen content determination of 0.89 ppm.

Evaluating cold cracking susceptibility requires a quantitative cold cracking criterion. This criterion is used to assess local factors influencing cold cracking susceptibility and has been determined using the S-TRC test (simulated tensile restraint cold cracking test) according to [12]. In this test, tensile specimens, illustrated on the left in Figure 2, are subjected to a specific loading process in an H2 gas atmosphere. They undergo various temperature cycles similar to the welding process and are tensile-loaded during cooling within the cold cracking critical temperature range, ultimately leading to cold cracking at a specific initiation temperature and stress. Temperature cycles with varying heating rates, maximum temperatures, and cooling times are used to set critical microstructures (hardness). Each crack initiation experiment represents a critical point of the resulting cold crack criterion, which describes the critical stresses as a function of the parameters: heating rate, maximum temperature, cooling time and hydrogen concentration. The criterion is valid for a range of these factors and has been determined using the Gleeble 3500 test and simulation center.

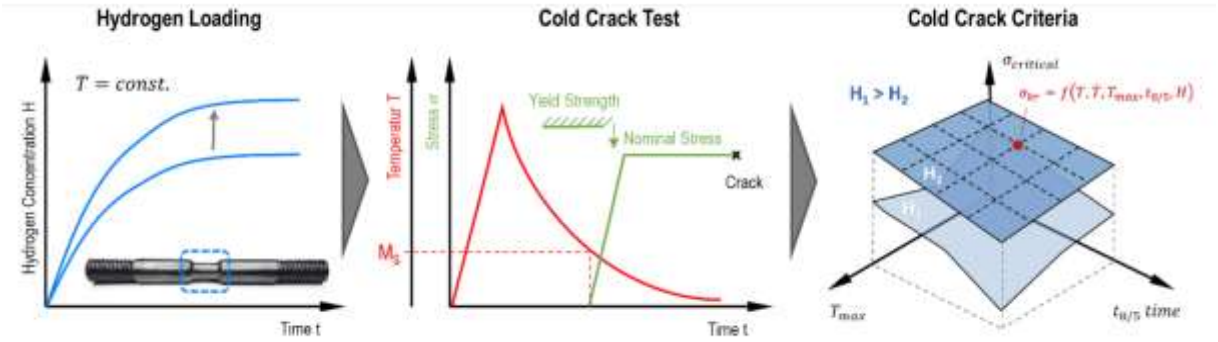

Fig. 2. Characteristics of hydrogen loading, cold crack test and cold crack criterion

Welding tests with active axial force control range of ± 2kN as well as with superimposed tilting moments (-1,5 °< □ < 1,5 °) were carried out using a specially manufactured clamping device from Föhrenbach GmbH.

FE Simulation

The weld temperature cycle forms the foundation for the development of cold crack-critical residual stresses and distortions. The heat input is represented using a heat conduction model, which includes a superposition of a normally distributed circular surface and a conical volume source [21–23]. Both thermophysical and thermomechanical material properties were implemented as a function of temperature and microstructure. The transformation temperatures determined in dilatometer tests were considered for different maximum temperatures and cooling times. The microstructure influences the resulting stresses, strains and hydrogen concentrations due to accompanying changes in physical properties. The superposition of shrinkage and transformation stresses leads to different residual stress distributions. Since the transformation stresses depend on the microstructural transformations [24–31], the stress formation can only be considered in conjunction with the microstructural transformation. Hydrogen diffusion in turn depends on the stress and strain state. The Leblond-Devaux [32] microstructure model was used for austenite formation and the Koistinen-Marburger [33] transformation kinetics for hardening martensite microstructure formation. For the thermo-mechanical calculations, microstructure specific thermal expansion, Young's modulus and yield strength were considered. The corresponding stress-strain curves for calibrating the material model were determined in hot tensile tests for various maximum temperatures and cooling times in the Gleeble 3500 test and simulation center. Hydrogen diffusion is influenced by temperature fields, microstructure and stress gradients. During welding a distribution occurs which also depends on the boundary conditions. The initial hydrogen content of the weld specimens is the initial condition of the calculation.

Cold crack prediction

Cold cracking at various temperatures is influenced by three interrelated factors: microstructure, hydrogen concentration and stress-strain state [26], [34]. Cold cracking is determined by the combination of locally critical values of these factors and is defined by exceeding the locally critical stress. F igure 1 illustrates the connection between the FE simulation and the cold crack tool. The cold crack criterion is incorporated into the cold crack tool as a material-specific criterion, providing an interpolation space for calculating critical stresses. For each node or element of the weld and heat-affected zone, and for each time step, a comparison can be made between the calculated and experimentally determined critical stresses. The Cold Crack tool has been integrated into the autonomous calculation process using batch file control, allowing for the variation of different control concepts in the simulation.

Results and Discussions

Influence of clamping (without using the dynamic axes of the clamping device)

The mechanical boundary conditions (Figure 3) have a significant influence on the plasticity during welding. The resulting stresses and distortions are determined by the expansion and the amount

of plastic strain. First, the influence of the clamping stiffness and the free clamping length were analyzed for their effect on the distortion. For a stiffness of 1000 N/m, variation calculations of the clamping length were carried out.

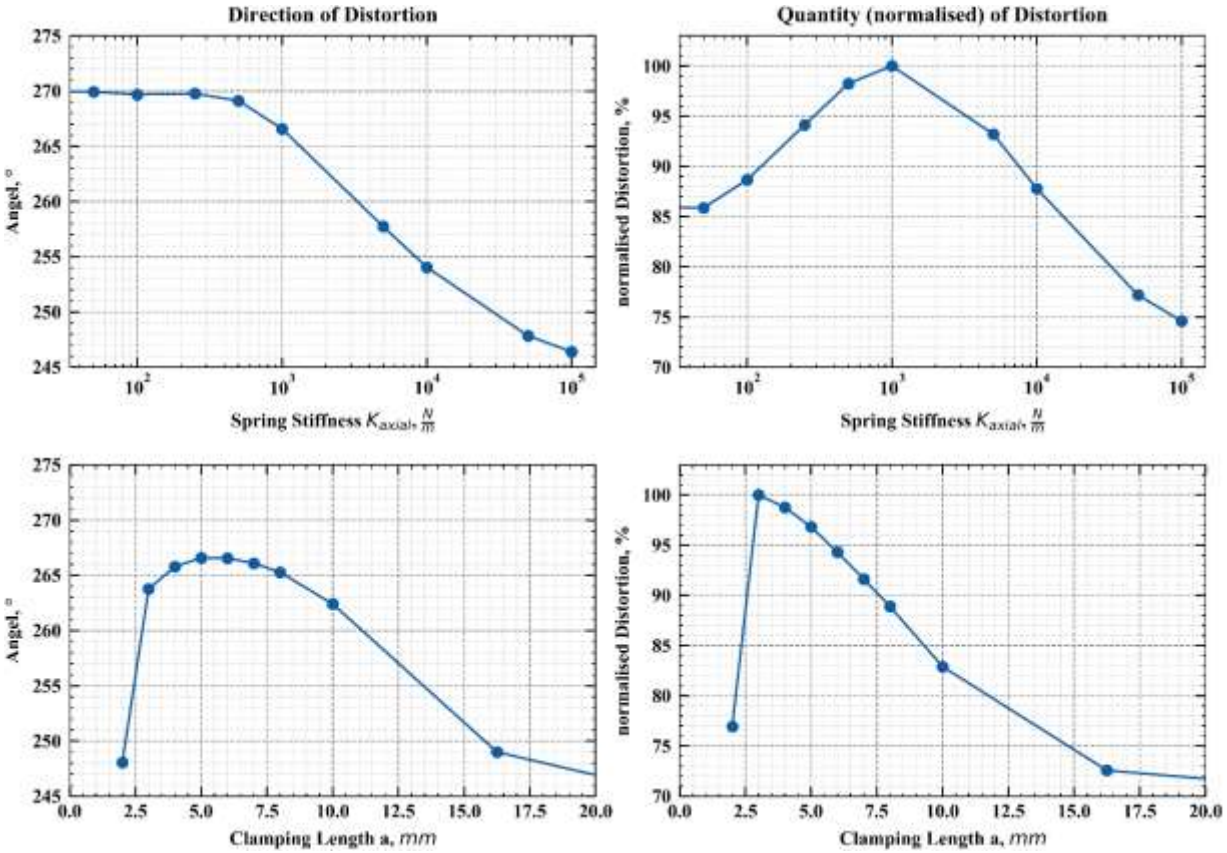

Fig. 3. Effect of clamping stiffness (top) and free clamping length between jaws on distortion (bottom)

The top section of Figure 3 demonstrates that the stiffness of the restraint influences both the height and direction of the distortion. As stiffness increases, there is a noticeable change in the distortion direction by up to 24° and a reduction in distortion height. Maximum distortion occurs at a stiffness of approximately 10^3 N/m. For a spring stiffness of 10^5 N/m, the distortion measured in the welding tests could be replicated. The impact of the free clamping length between the jaws on distortion is depicted in the bottom section of the figure. A reduction in distortion of up to 30% was calculated as the free clamping length increased. Both variations exhibit a change in the direction of distortion. This reveals a local shift of the plasticity maxima in relation to the welding angle.

First Simulation Scenario

The first simulation scenario aims to reduce distortion by applying controlled axial forces with the dynamic clamping system during welding. According to this concept, plastic strains are to be compensated by a counterforce. Variation calculations were conducted to examine the extent to which the magnitude of axial force applied impacts distortion. Since the investigations revealed that the timing of force application is influenced by the welding angle, the force application phase was also adjusted accordingly.

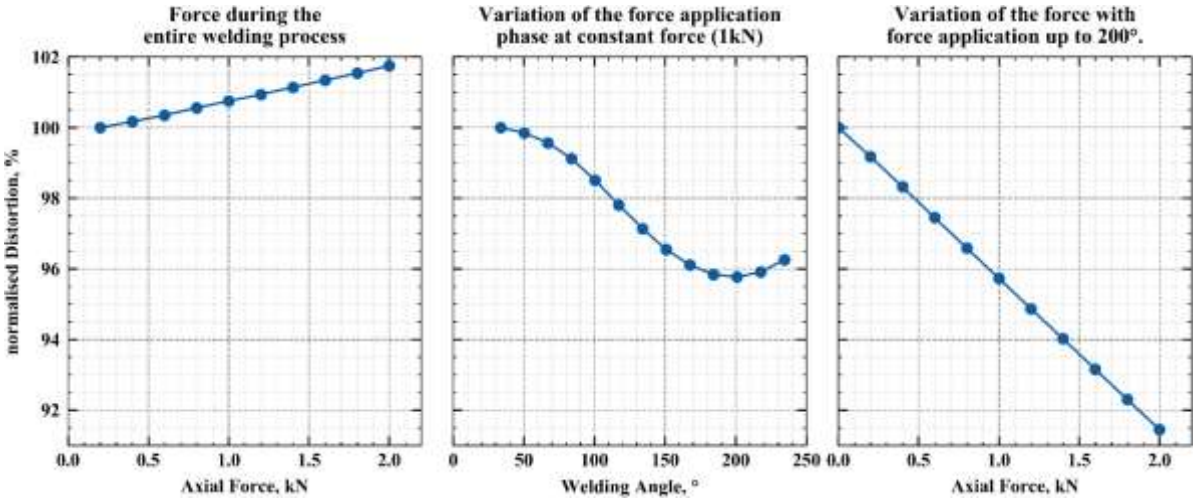

Fig. 4. Variation calculations with increasing axial force (pressure) throughout the welding process

Figure 4 demonstrates that a linear increase in distortion occurs as a function of axial force when the force is applied throughout the entire welding process (Fig. 4a). In subsequent simulations (Fig. 4b), the temporal force application phase during welding, expressed by the welding angle achieved at force application, was varied. The results indicate that distortion reaches a minimum at a force application of approximately 200° welding angle. This measure leads to a reduction in distortion compared to welding without force application. Lastly, for the calculated minimum of 200° welding angle, a variation of the axial force was performed (Fig. 4c). As the axial force increased (up to the maximum force of 2 kN), distortion was reduced by roughly 10%.

Tactile distortion measurements on reference specimens (Fig. 6a) without dynamic clamping revealed an average distortion of approximately 30 µm and a distortion direction of about 335°. The application of axial force during welding (Figure 6b) results in the elastic compression of the specimens, causing the joint to move out of the laser focus. As the force is applied as described up to a welding angle of 200°, the center of the weld is displaced during the welding process. A control routine was implemented to adjust the laser focus with a scanner optic as a function of the process time.

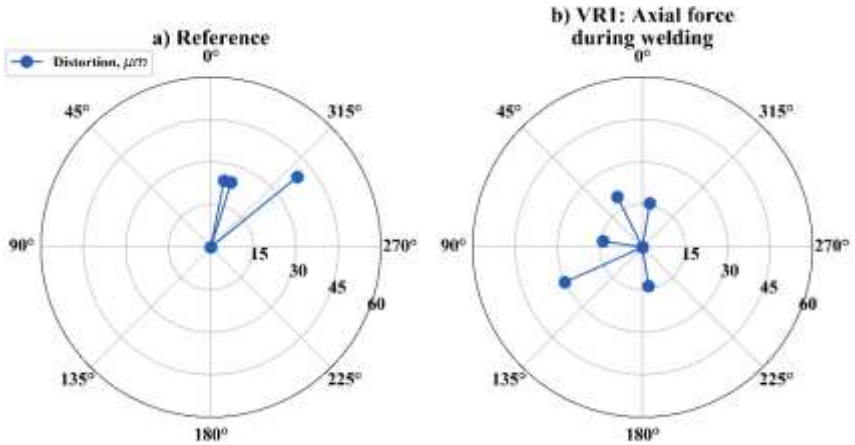

Fig. 5. Distortion measurements after welding tests

In test series 1, a reduction in distortion was achieved compared to the reference specimens, but the direction of distortion fluctuated greatly, possibly due to the formation of cold cracks. As cracks form, local stresses relax, resulting in undefined changes in the distortion angle.

Second Simulation Scenario

In the second simulation scenario, a bending element is used to reduce distortion by tilting the axis against the direction of the distortion. The objective is to bend the specimen and compensate any

existing distortion. Figure 6 shows a case where the distortion occurs at a 270° angle. To correct the distortion, the bending element must be tilted in the opposite direction, towards 90°. However, the exact direction of the distortion is not known at first, as it occurs after welding. It must be determined through simulations or measurements during or after the welding process. To ensure the best results, the bending element is activated immediately after welding (1 second post-welding) to align the rotary axis and maximize deformability at the highest component temperature. The simulation outcome is obtained by adjusting the bending angle, as shown in Figure 6.

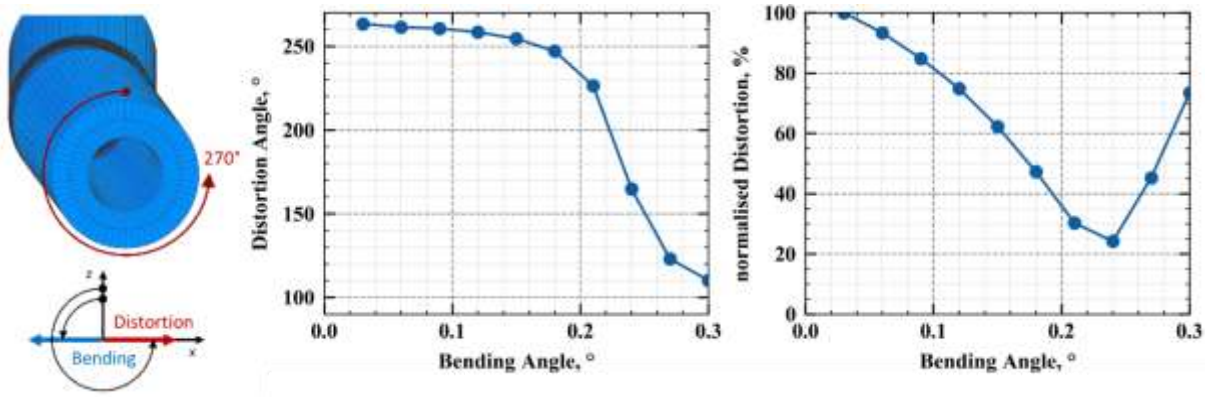

Fig. 6. Bend angle variation

To reduce the distortion in the direction of the x-axis (270°) by approximately 80%, a bending angle of 0.24° must be applied in the opposite direction. The remaining final distortion occurs at an angle of about 160°.

Third Simulation Scenario

The third simulation scenario addresses cold cracking reduction. Axial compressive forces are introduced to decrease tensile stresses, similar to the method used for distortion reduction. The external stress during cooling temporarily reduces lattice strains and local hydrogen concentration, slowing down hydrogen-induced embrittlement at low temperatures and enhancing the material's technological strength during cooling. To study the impact of these factors on cold cracking, simulations were run with a constant axial force of 2 kN for 1 to 60 seconds after welding.

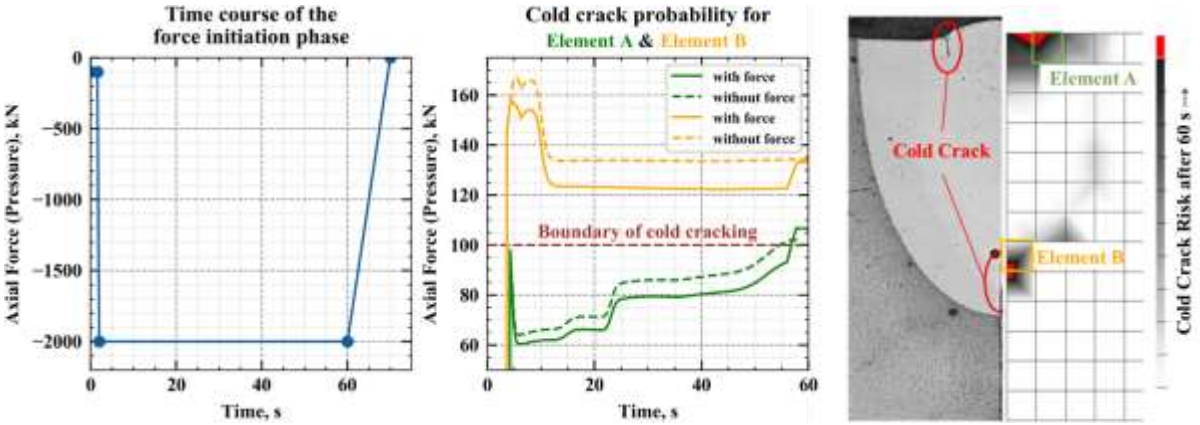

Fig. 7. Axial force after welding to reduce the tendency to cold cracking

Figure 7 illustrates the evolution of cold cracking tendency from welding to the release of the specimen after 60 seconds. The right part of the figure displays the local distribution of cold cracking tendency (at 60s) on the bottom section of a specimen welded without force (reference test). The simulation results demonstrate good consistency with the experiment for predicting cold cracks. The cracked weld areas in the simulation exhibit a high tendency for cold cracking (represented by red elements). By applying an axial force post-welding, it was possible to reduce the cold cracking ten-

dency at critical points of the weld, although the reduction was not enough to bring element B into a subcritical state. However, since not all crack locations exceed the allowable stress, it can be concluded that this measure reduces the frequency of cracks.

Conclusions

This research examined the impact of active force control during the Laser Beam Welding (LBW) on reducing distortion and cold cracking in high-strength steel 100Cr6. Finite Element (FE) simulations were utilized to model the welding process, considering the temperature field, microstructure changes, residual stresses and hydrogen distribution. Three simulation scenarios were investigated: the application of controlled axial forces, the use of a bending element with dynamic clamping, and reducing cold cracking tendencies.

The main conclusions are:

- Dynamic clamping in the Laser Beam Welding (LBW) process significantly reduces distortion and cold cracking, improving the weldability of high-strength materials through active control.
- The Finite Element (FE) welding process simulations, which consider temperature fields, microstructure changes, residual stresses, and hydrogen diffusion, provide accurate calculations of distortion and evaluations of cold cracking susceptibility
- Applying varying axial forces during welding can notably decrease distortion and cold cracking tendencies in welded specimens.
- The use of simulation models enables replacing costly experiments with virtual methods, reducing development times and enabling the derivation of optimal welding parameters and control concepts.
- The developed approaches and simulation models can be applied to various weld geometries and materials, optimizing weld properties and enabling the development of design-oriented control concepts.

The implementation of these conclusions in industrial settings will lead to a reduction in local cold cracking and distortion, thereby enhancing process reliability. Furthermore, the simulation models facilitate product development by substituting expensive experiments with suitable virtual methods, significantly decreasing development times. This approach enables the derivation of optimal welding parameters and control concepts for various weld geometries and materials. Consequently, weld properties can be optimized across diverse materials, and design-oriented control concepts can be established for a broader range of applications.

Funding and Acknowledgements

The authors acknowledge the financial support provided by the German Federal Ministry of Education and Research (BMBF) through the joint project "SimCoLas - Simulation Controlled Laser Welding". (Funding reference 13N13832).

Literature

[1] S. Katayama, *Fundamentals and details of laser welding*. in Topics in mining, metallurgy and materials engineering. Singapore: Springer, 2020.

[2] W. M. Steen and J. Mazumder, *Laser Material Processing*. London: Springer London, 2010. doi: 10.1007/978-1-84996-062-5.

[3] D. Coviello *et al.*, “Laser welding of tailored blanks made of Al-Si-coated 22MnB5 steel using a filler wire and a variable energy distribution laser optics,” *Int J Adv Manuf Technol*, vol. 125, no. 5–6, pp. 2691–2704, Mar. 2023, doi: 10.1007/s00170-023-10921-4.

[4] S. S. Nayak, E. Biro, and Y. Zhou, “Laser welding of advanced high-strength steels (AHSS),” in *Welding and Joining of Advanced High Strength Steels (AHSS)*, Elsevier, 2015, pp. 71–92. doi: 10.1016/B978-0-85709-436-0.00005-9.

[5] P. Wen, D. Yelkenci, J. Chen, B. Chang, D. Du, and J. Shan, “Numerical analysis of the effect of welding positions on formation quality during laser welding of TC4 titanium alloy parts in aerospace industry,” *Journal of Laser Applications*, vol. 31, no. 2, p. 022401, May 2019, doi: 10.2351/1.5096095.
[6] K. Fahlström, O. Andersson, U. Todal, and A. Melander, “Minimization of distortions during laser welding of ultra high strength steel,” *Journal of Laser Applications*, vol. 27, no. S2, p. S29011, Feb. 2015, doi: 10.2351/1.4906468.
[7] P. D. Babu, P. Gouthaman, and P. Marimuthu, “Effect of Heat Sink and Cooling Mediums on Ferrite Austenite Ratio and Distortion in Laser Welding of Duplex Stainless Steel 2205,” *Chin. J. Mech. Eng.*, vol. 32, no. 1, p. 50, Dec. 2019, doi: 10.1186/s10033-019-0363-5.
[8] K. Schricker, L. Schmidt, H. Friedmann, and J. P. Bergmann, “Gap and Force Adjustment during Laser Beam Welding by Means of a Closed-Loop Control Utilizing Fixture-Integrated Sensors and Actuators,” *Applied Sciences*, vol. 13, no. 4, p. 2744, Feb. 2023, doi: 10.3390/app13042744.
[9] T. Schaupp, W. Ernst, H. Spindler, and T. Kannengiesser, “Hydrogen-assisted cracking of GMA welded 960 MPa grade high-strength steels,” *International Journal of Hydrogen Energy*, vol. 45, no. 38, pp. 20080–20093, Jul. 2020, doi: 10.1016/j.ijhydene.2020.05.077.
[10] J. D. Velasquez, B. T. Alexandrov, and S. L. McCracken, “Hydrogen Induced Cracking Susceptibility in the Heat Affected Zone of SA-508 Pressure Vessel Steel,” in *Volume 4B: Materials and Fabrication*, Las Vegas, Nevada, USA: American Society of Mechanical Engineers, Jul. 2022, p. V04BT06A008. doi: 10.1115/PVP2022-84781.
[11] T. Kannengiesser and T. Boellinghaus, “Cold cracking tests—an overview of present technologies and applications,” *Weld World*, vol. 57, no. 1, pp. 3–37, Feb. 2013, doi: 10.1007/s40194-012-0001-7.
[12] O. Dreibati, *Physical welding simulation of the cold crack susceptibility: = Physikalische Schweißsimulation der Kaltrissanfälligkeit*. in Berichte des Lehrstuhls Füge- und Schweißtechnik der BTU Cottbus-Senftenberg, no. 8. Aachen: Shaker, 2014.
[13] E. Steppan, T. Mente, and Th. Böllinghaus, “Numerical investigations on cold cracking avoidance in fillet welds of high-strength steels,” *Weld World*, vol. 57, no. 3, pp. 359–371, May 2013, doi: 10.1007/s40194-013-0036-4.
[14] W. Zhao, M. Yang, T. Zhang, Q. Deng, W. Jiang, and W. Jiang, “Study on hydrogen enrichment in X80 steel spiral welded pipe,” *Corrosion Science*, vol. 133, pp. 251–260, Apr. 2018, doi: 10.1016/j.corsci.2018.01.011.
[15] A. Díaz, I. I. Cuesta, C. Rodríguez, and J. M. Alegre, “Influence of non-homogeneous microstructure on hydrogen diffusion and trapping simulations near a crack tip in a welded joint,” *Theoretical and Applied Fracture Mechanics*, vol. 112, p. 102879, Apr. 2021, doi: 10.1016/j.tafmec.2020.102879.
[16] M. Rhode, T. Mente, E. Steppan, J. Steger, and T. Kannengiesser, “Hydrogen trapping in T24 Cr-Mo-V steel weld joints—microstructure effect vs. experimental influence on activation energy for diffusion,” *Weld World*, vol. 62, no. 2, pp. 277–287, Mar. 2018, doi: 10.1007/s40194-017-0546-6.
[17] T. Boellinghaus and E. Viyanit, “Numerical Simulations of Hydrogen-Assisted Cracking in Girth Welds of Supermartensitic Stainless Steel Piplines - Report I,” *Mathematical modelling of weld phenomena. 6, Institute of Materials, Minerals and Mining*, 2002.
[18] TH. Boellinghaus, E. Viyanit, and H. Hoffmeister, “Numerical Simulations of Hydrogen-Assisted Cracking in Girth Welds of Supermartensitic Stainless Steel Piplines - Report II,” in *Mathematical modelling of weld phenomena. 7*, Verl. der Techn. Univ. Graz, 2005.
[19] M. Stadtaus, H. Wohlfahrt, K. Dilger, and V. Michailov, “Numerical Simulations of the Tekken-Test for the Prediction of Cold Cracking Susceptibility,” in *Mathematical modelling of weld phenomena. 7*, Verl. der Techn. Univ. Graz, 2005.
[20] M. Stadtaus, N. Doynov, and V. Michailov, “Investigation of the modified CTS-Test for the Prediction of Cold Cracking Suscepibility by Numerical Models,” in *Mathematical modelling of weld phenomena. 8*, Graz: Verl. der Techn. Univ. Graz, 2007.
[21] N. N. Rykalin, *Berechnung der Wärmevorgänge beim Schweissen*. 1957.

[22] J. Goldak, A. Chakravarti, and M. Bibby, “A new finite element model for welding heat sources,” *MTB*, vol. 15, no. 2, pp. 299–305, Jun. 1984, doi: 10.1007/BF02667333.
[23] N. T. Nguyen, *Thermal analysis of welds*. in International series on developments in heat transfer, no. v. 14. Southampton ; Boston: WIT, 2004.
[24] R. Ossenbrink and V. Michailov, “Thermomechanical Numerical Simulation with the Maximum Temperature Austenisation Cooling Time Model (STAAZ),” *Verlag der Technischen Universität Graz*, vol. 8, pp. 357–372, 2007.
[25] B. T. Alexandrov, “Hydrogen Behaviour in welded joints and evaluation of its role for cold cracking,” *Verlag der Technischen Universität Graz*, vol. 7, pp. 781–804, 2005.
[26] T. Boellinghaus and H. Hoffmeister, “Finite element calculations of pre- and post-heating procedures for sufficient hydrogen removal in butt joints,” *Verlag der Technischen Universität Graz*, vol. 3, pp. 726–756, 1997.
[27] V. Michailov, K. Thomas, and H. Wohlfart, “Numerische Simulation der Wasserstoffverteilung in mehrlagigen Schweißverbindungen,” *Schweißen und Schneiden*, no. 48, pp. 47–54, 1996.
[28] V. Michailov, K. Thomas, and H. Wohlfart, “Ermittlung der Wasserstoffverteilung in Schweißverbindungen mit der Finite-Elemente-Methode,” *DVS-Berichte*, vol. 156, pp. 167–171, 1993.
[29] M. Stadtaus and V. Michailov, “Numerische Berechnung der Einflußfaktoren auf die Kaltrissbildung,” *Materialwissenschaft und Werkstofftechnik*, vol. 34, 2003.
[30] M. Neuhaus, T. Kannengiesser, and T. Boellinghaus, “Beurteilung der Kaltrisssicherheit von Schweißverbindungen in realen Konstruktionen mit der Finite-Elemente-Methode,” *DVS-Berichte*, vol. 232, pp. 195–200, 2004.
[31] H. Wohlfahrt, “Die Bedeutung der Austenitumwandlung für die Eigenspannungsentstehung beim Schweißen,” *Härterei Technische Mitteilungen*, vol. 41, pp. 248–257, 1986.
[32] J. B. Leblond and J. Devaux, “A new kinetic model for anisothermal metallurgical transformations in steels including effect of austenite grain size,” *Acta Metallurgica*, vol. 32, no. 1, pp. 137–146, Jan. 1984, doi: 10.1016/0001-6160(84)90211-6.
[33] D. P. Koistinen and R. E. Marburger, “A general equation prescribing the extent of the austenite-martensite transformation in pure iron-carbon alloys and plain carbon steels,” *Acta Metallurgica*, vol. 7, no. 1, pp. 59–60, Jan. 1959, doi: 10.1016/0001-6160(59)90170-1.
[34] L. Yajiang, W. Juan, and S. Xiaoqin, “FEM calculation and effect of diffusion hydrogen distribution in the fusion zone of super-high strength steel,” *Computational Materials Science*, vol. 31, no. 1–2, pp. 57–66, Sep. 2004, doi: 10.1016/j.commatsci.2004.01.036.